MODEL BASED RECONSTRUCTION OF THE BONY KNEE ANATOMY FROM 3D ULTRASOUND IMAGES

Christoph Hänisch, Juliana Hsu, Erik Noorman, Klaus Radermacher

Chair of Medical Engineering, Helmholtz-Institute for Biomedical Engineering, RWTH Aachen University, Germany, haenisch@hia.rwth-aachen.de

INTRODUCTION

Nowadays, planning of image guided surgeries is often done using computed tomography (CT) and magnetic resonance imaging (MRI) (cf. Stiehl2005, Grimson1997). CT offers good image quality but due to its ionizing radiation it is invasive. Also, soft tissue is poorly visible in CT data. MRI is affected by distortions (Moro-oka2007) and quite expensive.

Ultrasound might serve as an alternative imaging modality. It offers high resolution images in real-time while being non-invasive, cost-effective and broadly available. Its weaknesses, however, are a low signal to noise ratio (SNR), speckle, low contrast, acoustic shadowing and a small field of view (FOV) (cf. Noble2006).

We developed an image processing chain as well as a related clinical workflow to reconstruct entire bone surfaces from 3D ultrasound volume data (see figure 1). A clinician acquires ultrasound images from relevant areas while scanning from various directions. The probe is tracked, the limb is equipped with non-invasive markers. The user is guided by a simple navigation interface in order to follow a standardized scanning process. Having acquired the necessary data, the volume images are segmented and registered to obtain a preliminary reconstruction. Due to acoustic shadowing, the reconstruction might be incomplete. However, incorporating a priori knowledge, the reconstruction can be completed. The applicability of our approach is demonstrated on the surface reconstruction of the distal femur.

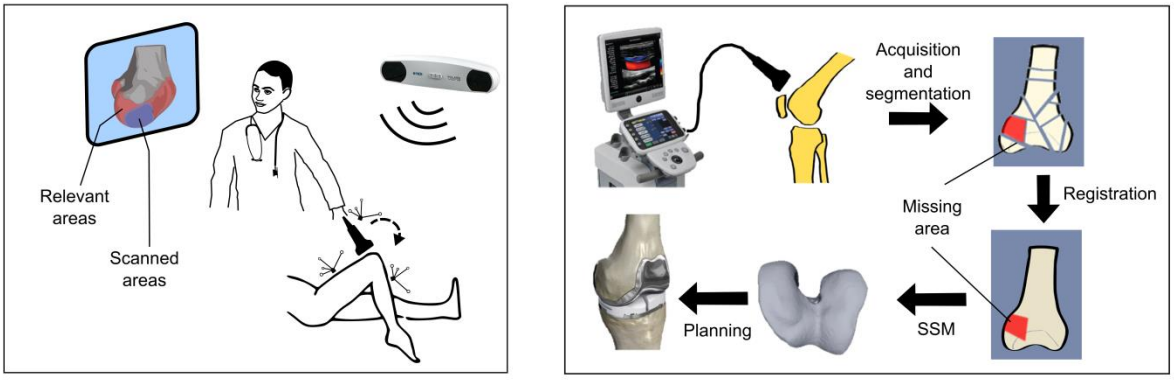

Figure 1: Clinical workflow and image processing chain.

MATERIALS AND METHODS

Data Acquisition

Various 3D ultrasound volume images of a solid foam bone phantom (*SAWBONES*) of the distal femur were acquired using the *Ultrasonix SonixTOUCH Research* system in combination with the linear array transducer 4DL14-5/38 (14 MHz). According to the protocol, the volume images were acquired from distinct directions with a slight overlap such that bone structures were located at the bottom side (see the segmentation section for more details). A

total of 19 images were recorded. The image data was stored as a series of 2D raw images which then were scan line converted to obtain volume images in Cartesian space.

Segmentation

The ultrasound volume images were segmented employing various level set methods (Osher1988). The basic idea behind this is that due to acoustic shadowing the inner region of the bone shows low intensity values. Thus, expanding an initial contour from inside yields the bone surface. Along the surface normal, the intensity profile is symmetric and the actual surface is expected to be between the point of highest gradient and highest intensity (cf. Jain2004).

The images were preprocessed by reverting the logarithmic compression and by applying an edge preserving median filter which reduces speckle and Gaussian noise. Assuming bone structures being located in the lower part of the image, initial level sets were estimated by traversing the image volumes column-wise and bottom up and searching for intensity values above a certain threshold level.

The initial level sets were optimized using a constrained variant of the distance regularized level set evolution (DRLSE) approach described by (Li2005). The level set evolutions had to be restricted in the border areas to prevent a gradual enclosing of the intensity profile if the structures did not fill up the entire image.

In a first optimization step, the evolution was carried out using a ridge detector based level set evolution as described in the original article by Li et al. In a second step, the edge indicator function was changed to a ridge indicator function incorporating 3D local phase features (Hacihaliloglu2009) which made use of the fact that the bone responses were symmetric.

The result of a level set evolution is a closed curve, thus, the final curves contained points that did not belong to the actual surfaces. These points were removed based on their locations and grey level values. Finally, triangle meshes were created from the level sets. The entire segmentation process is depicted in figure 2.

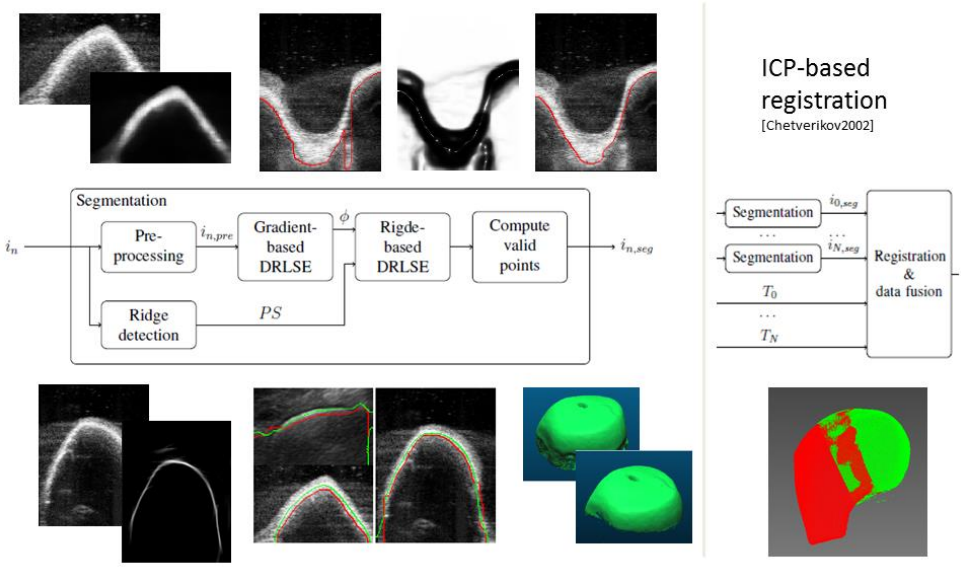

Figure 2: Stages of the level set based segmentation process of 3D ultrasound images. The images in the top row show a slice of an original volume image, its preprocessed image, an initial level set on an original image slice, its edge indicator function and the result of the gradient based DRLSE (from left to right). The bottom row shows a slice of an original volume image, the response of the ridge detector, initial level sets (red) on their original images and their refinements (green) and the resulting surfaces before and after removing uncertain surface points (from left to right).

Registration

The surface patches obtained in the segmentation process were taken to construct the bone surface geometry. Since no tracking information was available in this experimental set-up, first, the patches were aligned manually. Then a fine registration was carried out by selecting an initial reference patch and gradually registering the remaining surface patches from left to right. Since there was only a small overlap in the border areas of the patches, a variant of the iterative closest point (ICP) algorithm was used (Chetverikov2005).

Reconstruction

Due to acoustic shadowing, an incomplete distal femur geometry was obtained from the registration procedure. Two approaches were investigated to reconstruct the entire surface geometry. First, an average bone model was non-rigidly fitted to the surface (Amberg2007) incorporating local stiffness constraints to avoid leakage in areas without any surface information. Second, a statistical shape model (SSM) (cf. Heiman2009) was fitted to the incomplete surface geometry. The SSM is only allowed to deform within statistical limits based on some training data, thus always producing meaningful results.

The average bone model was constructed from 158 data sets being triangle meshes (10,000 vertices) of the distal femur surface obtained from CT data; the data was represented as point distribution models (PDM). First, an initial data set was selected randomly and fitted to the remaining data sets using the N-ICP-A algorithm (Amberg2007). Then, the resulting shape vectors were averaged. To avoid any bias from the selected initial data set, this scheme was repeated twice, each time using the previously computed mean shape as reference.

The SSM was constructed from the same 158 data sets. The point correspondences were established by fitting the mean shape to all data sets again employing the N-ICP-A. To fit the SSM to target geometries, an iterative procedure similar to that of active shape models (Cootes1995) was used. First, the mean shape was fitted to the target. Then, the resulting shape vector was projected into the parameter space and constrained to lie within three standard deviations. A new shape was constructed as a linear combination of the mean shape and the modes where the modes were weighted according to the parameter vector. Again, this new shape was fitted to the target. This procedure was repeated until convergence. We found, that three iterations were sufficient.

Validation

The segmentation process was validated by comparing the resulting bone surface patches individually with a ground truth obtained from a CT scan. The rough alignment was done manually and the fine registration was done by applying the iterative closest point algorithm. The validation was carried out in (CloudCompare2014). Similarly, the accuracy of the registration procedure was determined by comparing the entire registration result with the ground truth. Lastly, the reconstruction results were validated by comparing the bone morphing approach with the ground truth as well as the result obtained from the SSM approach.

RESULTS

All 19 ultrasound volume images could be successfully segmented. Fine details like small bumps and cavities were present. However, one of the patches exhibited a small extraneous segment in the border area which was removed. With this, the average distance error of all individually matched bone phantom patches was 0.30 mm ± 0.37 mm.

Due to acoustic shadowing, only part of the distal femur geometry could be scanned resulting in an incomplete surface reconstruction from the registration procedure. The surface registration error (SRE) between the ground truth and the surface reconstruction was 0.66 mm ± 0.55 mm.

The distal femur bone geometry could be successfully reconstructed using a morphing approach as well as by fitting a statistical shape model. Compared to the ground truth, the SRE of the morphing approach was 1.07 mm (absolute distances) and the average signed distance error was 0.77 mm ± 1.07 mm. The SRE of the SSM approach was 0.74 mm and the average signed distance error was -0.20 mm ± 0.95 mm. The results of the reconstruction process are shown in figure 3.

DISCUSSION

We developed an image processing chain to reconstruct entire bone surfaces from 3D ultrasound volume images. The fact that due to acoustic shadowing only part of the entire geometry is seen was addressed by incorporating a priori knowledge. With this, the average reconstruction error (SRE) was less than or equal to one millimeter compared to a ground truth obtained from CT data.

Within the framework, a new segmentation method was presented exhibiting submillimeter accuracy. The segmentation method was primarily based on level set methods. Local phase based features (Hacihaliloglu2009) were incorporated exploiting the fact that bone responses are symmetric (Jain2004). A similar approach was presented by (Belaid2011). However, Cauchy kernels were used instead of Log-Gabor filters to compute the asymmetry measure since they shall have better properties. Furthermore, their framework operates on 2D images only even though their methods might be extended to 3D.

In areas of low contrast, the curve evolution may be less controlled. This was especially observed at the border areas of the intensity profiles. To make the curve evolution more robust, statistical shape models could be incorporated (cf. Cootes1995, Tsai2003).

The surface patches obtained from the segmentation process were registered successively starting from an arbitrary initial data set. The disadvantage of this approach is that slight misregistrations may accumulate and finally lead to a drift. Multiview registration techniques may yield better registration results.

A priori knowledge was incorporated in the form of a statistical mean shape (SSM) or simply by fitting average bone geometries. Compared to simple morphing, SSM have the desirable property of being specific, that is, their morphology changes only within statistical limits based on training samples.

While constructing the SSM, point correspondences must be established. Referring to (Heiman2009), the minimum description length approach (MDL) yields the best results. The MDL algorithm estimates all correspondences at once, thus obeying a time complexity of $O(n^2)$. Using 158 training data sets with about 10.000 points, employing the MDL approach was not feasible. Instead, we fitted a reference shape (we used the mean shape) to all data sets one after another which is of O(n) using the ICP variant of (Amberg2007). The advantage of this new approach is not only the lower time complexity, but the possibility to add more training data sets at a later point in time.

As discussed above, the SSM based approach yielded better results than the morphing based approach. However, this depends on the *completeness* of the underlying data. The more complete the base data, the better performs the morphing approach since it can deform without

any restrictions. But if only few base data is available, the SSM clearly outperforms the morphing approach since the missing information is inherent in the statistics.

In conclusion, we developed a new method to reconstruct entire bone surfaces from ultrasound images with an average reconstruction error (SRE) less than or equal to one millimeter. Incorporating a priori knowledge (e.g. in the form of statistical shape models), we were able to reconstruct areas that were not present in the base data. Furthermore, we presented a new method for segmenting image patches with submillimeter accuracy.

ACKNOWLEDGEMENT

Parts of this work were co-funded by the German federal state North Rhine Westphalia (NRW) and the European Union (European Regional Development Fund: Investing In Your Future), grant No. 005- 1111-0047, PtJ-Az.: z1104me029a.

REFERENCES

- Amberg B, Romdhani S, Vetter T, Optimal Step Nonrigid ICP Algorithms for Surface Registration, CVPR, pp. 1 – 8, 2007
- Belaid A et al., Phase-Based Level Set Segmentation of Ultrasound Images, Information Technology in Biomedicine, Vol. 15, No. 1, 2011
- Chetverikov D, Stepanov D and Krsek P, Robust Euclidean alignment of 3D point sets: The trimmed iterative closest point algorithm, Image and Vision Computing, Vol. 23, No. 3, pp. 299 – 309, 2005
- CloudCompare (version 2.5) [licensed under GPL], EDF R&D, Telecom ParisTech, http://www.cloudcompare.org/, 2014
- Cootes TF et al., Active Shape Models - Their Training and Application, Computer Vision and Image Understanding, Vol. 61, No. 1, pp. 38 – 59, 1995
- Grimson WEL et al., Utilizing Segmented MRI Data in Image-Guided Surgery, IJPRAI, Vol. 11, No. 8, pp. 1367 – 1397, 1997
- Hacihaliloglu I and others, Automatic Data-Driven Parameterization for Phase-Based Bone Localization in US Using Log-Gabor Filters, ISVC, Part I, LNCS 5875, pp. 944 – 954, 2009
- Heimann T, Meinzer HP, Statistical shape models for 3D medical image segmentation: A review, Medical Image Analysis, Vol. 13, No. 4, pp. 543 – 563, 2009
- Jain AK, Taylor RH, Understanding Bone responses in B-mode Ultrasound Images and Automatic Bone Surface extraction using a Bayesian Probabilistic Framework, Proc. of SPIE, Vol. 5373, pp. 131 – 142, 2004
- Li C and others, Level Set Evolution Without Re-initialization: A New Variational Formulation, CVPR, Vol. 1, pp. 430 – 436, 2005
- Osher S, Sethian JA, Fronts propagating with curvature-dependent speed: algorithms based on Hamilton-Jacobi formulations, Journal of Computational Physics, Vol. 79, No. 1, pp. 12 – 49, 1988
- Moro-oka et al., Can Magnetic Resonance Imaging–Derived Bone Models Be Used for Accurate Motion Measurement With Single-Plane Three-Dimensional Shape Registration?, Journal of Orthopaedic Research, Vol. 25, No. 7, pp. 867 – 872, 2007
- Noble JA, Boukerroui D, Ultrasound Image Segmentation: A Survey, Medical Imaging, Vol. 25, No. 8, pp. 987 – 1010, 2006

- Stiehl JB, Konermann WH, Haaker RG, Computer-Assisted Surgery: Principles, Total Knee Arthroplasty, pp. 241 – 246, 2005
- Tsai A et al., A Shape-Based Approach to the Segmentation of Medical Imagery Using Level Sets, Medical Imaging, Vol. 22, No. 2, pp. 137 – 154, 2003

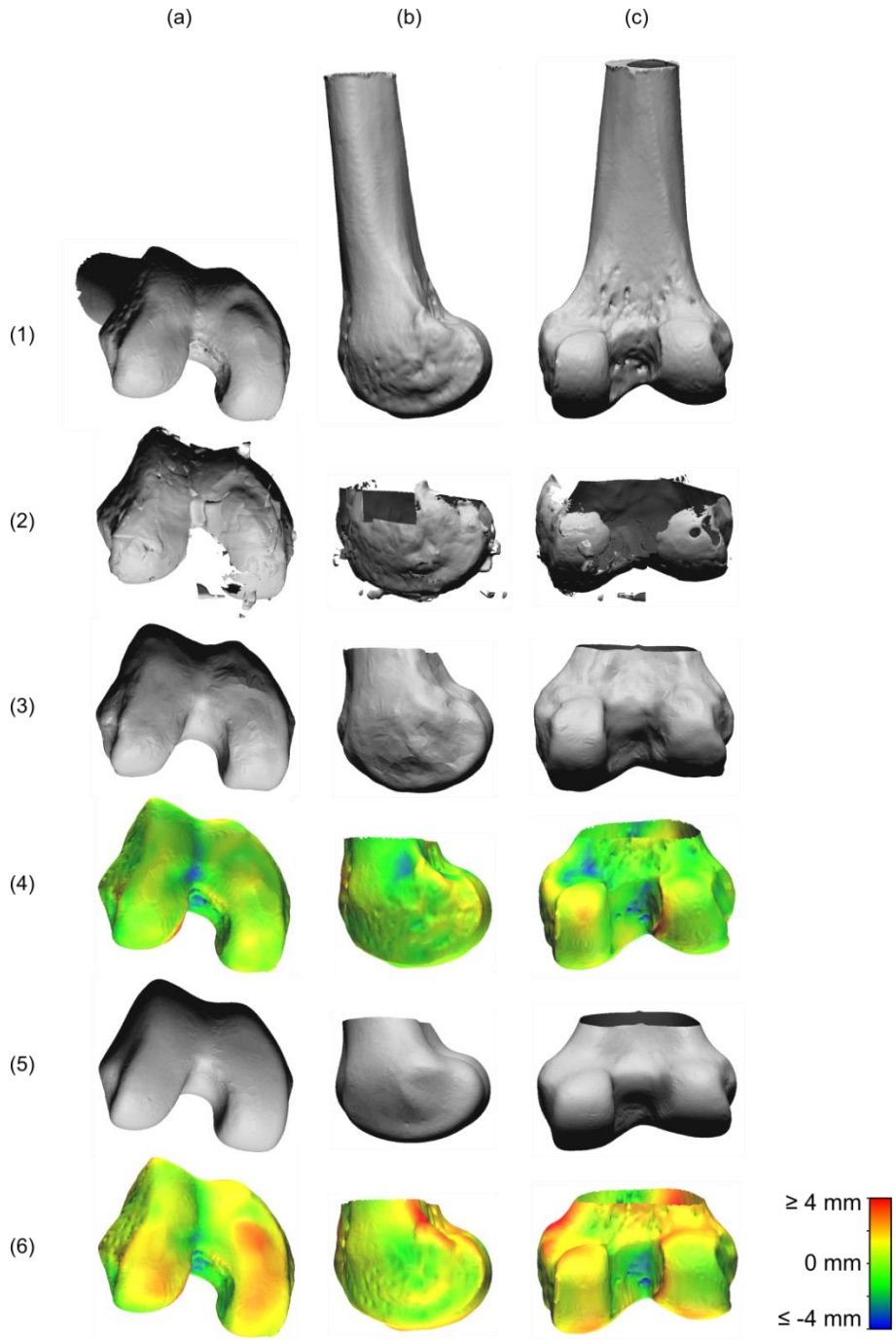

Figure 3: Various views of a solid foam femur model are shown. Illustrated are: (1) the CT based reconstruction (ground truth), (2) the registration result from the segmented patches, (3)-(4) the SSM based reconstruction, (5)-(6) the result of the non-rigidly fitted mean shape.